Morphology Control of Zinc Oxide Particles at Low Temperature

ARTICLE *in* CRYSTAL GROWTH & DESIGN · AUGUST 2008

Impact Factor: 4.89 · DOI: 10.1021/cg060607c

2 AUTHORS, INCLUDING:

Yoshitake Masuda
National Institute of Advanced Industrial S…
306 PUBLICATIONS **5,489** CITATIONS

CRYSTAL GROWTH & DESIGN
2008
VOL. 8, NO. 8
2633–2637

Articles

Morphology Control of Zinc Oxide Particles at Low Temperature

Yoshitake Masuda* and Kazumi Kato

National Institute of Advanced Industrial Science and Technology (AIST), 2266-98 Anagahora, Shimoshidami, Moriyama-ku, Nagoya 463-8560, Japan

Received September 12, 2006; Revised Manuscript Received December 3, 2007

ABSTRACT: We controlled the crystal growth of ZnO to realize morphology control of ZnO particles and particulate films. Crystalline ZnO was nucleated in aqueous solutions containing zinc nitrate hexahydrate and ethylenediamine at 60 °C. ZnO particles had many needles and Ultrafine surface relief structures. ZnO particles then deposited on substrates to form particulate films, and thin sheets were further grown to connect ZnO particles to each other and with substrates. Crystal growth control and morphology control of ZnO in aqueous solutions would contribute to the development of crystallography of oxide materials in solutions and future inorganic devices such as sensors and solar cells.

Introduction

ZnO has attracted much attention as a next-generation gas sensor for CO,[1–3] NH_3,[4] NO_2,[5] H_2S,[6] H_2,[2,7] ethanol,[7,8] SF_6,[7] C_4H_{10},[7] or gasoline[7] and dye-sensitized solar cells.[9–13] Sensitivity directly depends on the specific surface area of the sensing material. ZnO particles, particulate films, or mesoporous materials having high specific surface area were thus strongly required.

ZnO has been crystallized to a hexagonal cylinder shape for gas sensors or solar cells in many studies[9] by using the hexagonal crystal structure of ZnO at low supersaturation degree. However, strategic morphology design and precise morphology control for high specific surface area should be developed to improve the properties. ZnO particles should be controlled to have multineedles or high surface asperity to increase the specific surface area by the crystallization at high supersaturation degree.

Recently, morphology control[14–17] and nano/micro manufacturing[18–21] of oxide materials were proposed in solution systems. Solution systems have the advantage of adjustment of supersaturation degree and high uniformity in the system for particle morphology control. However, many factors affect the system compared to gas phase systems or solid-state reactions. Solution chemistry for oxide materials is therefore being developed, and many areas remain to be explored.

We recently proposed morphology control of ZnO particles to hexagonal cylinder shape, ellipse shape, and multineedle shape.[14] Photoluminescence property was improved by changing the morphology and oxygen vacancy volume in this system. Morphology control of ZnO has also been proposed based on control of crystal growth.[22–25] Peng et al. reported flower-like bunches synthesized on indium-doped tin oxide glass substrates through a chemical bath deposition process.[22] Lin et al. fabricated nanowires on a ZnO-buffered silicon substrate by a hydrothermal method.[23] Zhang et al. prepared flowerlike, disklike, and dumbbell-like ZnO microcrystals by a capping-molecule-assisted hydrothermal process.[24] Liu et al. reported a hierarchical polygon prismatic Zn-ZnO core−shell structure grown on silicon by combining liquid-solution colloidals together with the vapor−gas growth process.[25] These studies showed high morphology controllability of ZnO; however, morphology should be optimized to have high specific surface area to apply to solar cells or gas sensors.

In this study, we proposed the morphology design of ZnO particles for solar cells or gas sensors in which high specific surface area, high electrical conductivity, and high mechanical strength are required and fabricated multineedle ZnO particles having Ultrafine surface relief structure, as well as particulate films constructed from multineedle particles and thin sheets. Morphology control was realized based on a new idea inspired from the morphology change in our former study.[14] High supersaturation degree of the solution was used for fast crystal growth which induces the formation of multineedle particles and low supersaturation was used for the formation of ZnO thin sheets.

Experimental Section

Morphology Control of ZnO Particles. Zinc nitrate hexahydrate ($Zn(NO_3)_2 \cdot 6H_2O$, >99.0%, MW 297.49, Kanto Chemical Co., Inc.) and ethylenediamine ($H_2NCH_2CH_2NH_2$, >99.0%, MW 60.10, Kanto Chemical Co., Inc.) were used as received. Glass (S-1225, Matsunami Glass Ind., Ltd.) was used as a substrate. Zinc nitrate hexahydrate (15 mM) was dissolved in distilled water at 60 °C, and ethylenediamine (15 mM) was added to the solution to induce

* Corresponding Author: E-mail: masuda-y@aist.go.jp.

10.1021/cg060607c CCC: $40.75
Published on Web 06/20/2008

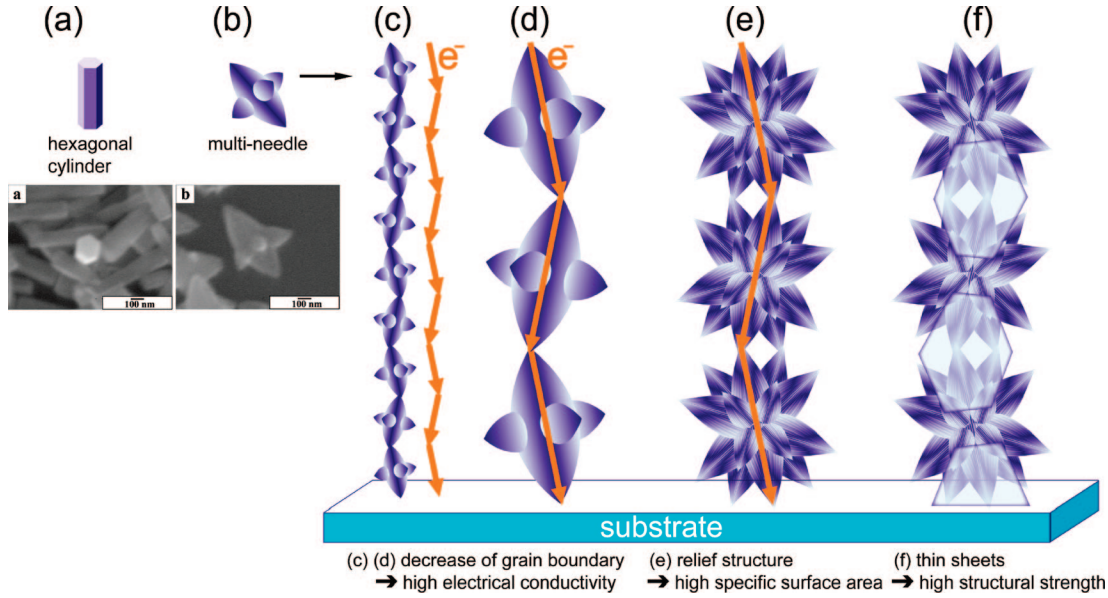

Figure 1. (a−f) Design and morphology control of ZnO particles and particulate films for high specific surface area, high electrical conductivity, and high mechanical strength.

the formation of ZnO. Glass substrate was immersed in the middle of the solution at an angle, and the solution was kept at 60 °C using a water bath for 80 min with no stirring. The solution became clouded shortly after the addition of ethylenediamine. Ethylenediamine plays an essential role in the formation of crystalline ZnO. ZnO was homogeneously nucleated and grown to form a large amount of particles to make the solution clouded. ZnO particles were gradually deposited and further grown on a substrate. Homogeneously nucleated particles precipitated gradually and the solution became light white after 80 min. The supersaturation degree of the solution was high at the initial stage of the reaction for the first 1 h and decreased as the color of the solution changed.

Morphology Control of ZnO Particulate Films. ZnO particulate films constructed from ZnO particles and thin sheets were fabricated by immersion for 48 h. The glass substrate was immersed in the middle of the solution at an angle and the solution was kept at 60 °C using a water bath for 6 h with no stirring. The solution was then left to cool for 42 h in the bath. The solution became clouded shortly after the addition of ethylenediamine and clear after 6 h. The bottom of the solution was covered with white precipitate after 6 h. The supersaturation degree of the solution was high at the initial stage of the reaction for the first 1 h and then decreased as the color of the solution changed.

Characterizations. Morphology of ZnO particles and particulate films was observed by a field emission scanning electron microscope (FE-SEM; JSM-6335FM, JEOL Ltd.) after heating at 150 °C for 30 min in vacuum for drying of carbon paste (Vacuum oven, VOS-201SD, EYELA, Tokyo Rikakikai. Co., Ltd.) and Pt coating for 3 nm (Quick cool coater, SC-701MCY, Sanyu Electronic Company). Crystal phases were evaluated by an X-ray diffractometer (XRD; RINT-2100V, Rigaku) with Cu Kα radiation (40 kV, 40 mA).

Results and Discussion

Morphology Design of ZnO Particles and Particulate Films. The morphology of ZnO particles was designed to increase the specific surface area, electrical conductivity, and mechanical strength of the base material of solar cells and sensors (Figure 1). Typical ZnO particles grown at low supersaturation degree are shown in Figure 1a.[14] The particles show edged hexagonal faces and elongate parallel to the *c*-axis. ZnO particles grew to have a hexagonal cylinder shape by slow crystal growth due to the hexagonal crystal structure of ZnO. The morphology of ZnO particles was controlled to have a multineedle shape in an aqueous solution (Figure 1b).[14] Multineedle particles have a high specific surface area compared to hexagonal cylinder particles, but particulate films constructed from small particles have many grain boundaries which reduce the electrical conductivity (Figure 1c). Particles should thus have large grain size to decrease grain boundaries and increase electrical conductivity (Figure 1d). Furthermore, the specific surface area of ZnO particles should be increased to improve the sensing performance of sensors or generating efficiency of solar cells (Figure 1e). An Ultrafine surface relief structure on ZnO particles is a candidate morphology for increasing the specific surface area. Additionally, particles should be connected to each other and with a substrate by a combined member such as ZnO thin sheets (Figure 1f). The thin sheets increase the mechanical strength of particulate films and help raise the electrical conductivity and specific surface area. Morphology control of ZnO particles was attempted based on the strategic morphology design for application to sensors.

Morphology Control of ZnO Particles. After having been immersed in the solution for 80 min, the substrate covered with ZnO particles was evaluated by SEM and XRD. ZnO particles were shown to be multineedle shape in which many needles were grown from the center of the particles (Figure 2). The particles have more needles compared with the particles previously reported which were constructed from two large needles and several small needles.[14] The size of particles was in the range of 1−5 μm, which is larger than the particles prepared previously[14] (Figure 1b). Needles were constructed from an assembly of narrow acicular crystals, and thus the side surfaces of needles were covered with arrays of pleats. The tips of the needles were rounded V-shape with many asperities. Edged hexagonal shapes were observed at the tips of needles, thus clearly showing high crystallinity and the direction of the *c*-axis. The *c*-axis would be the long direction of multineedles and narrow acicular crystals. Elongation of the *c*-axis observed by SEM is consistent with high diffraction intensity of 0002 (Figure 3). The 0002 diffraction intensity of multineedle ZnO particles was much stronger than 100 or 101 peaks though 0002 diffraction is weaker than 100 or 101 diffractions in randomly orientated ZnO particles (JCPDS No. 36-1451). High diffraction

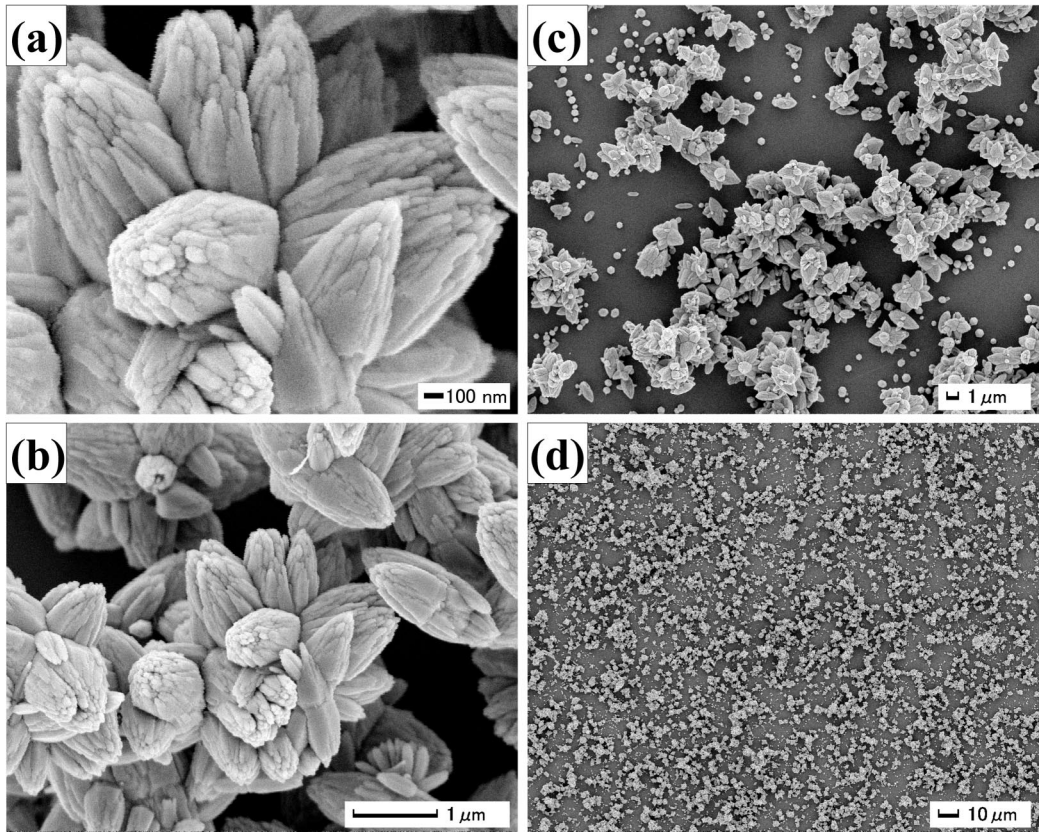

Figure 2. SEM micrograph (a−d) of multineedle ZnO particles having Ultrafine surface relief structure.

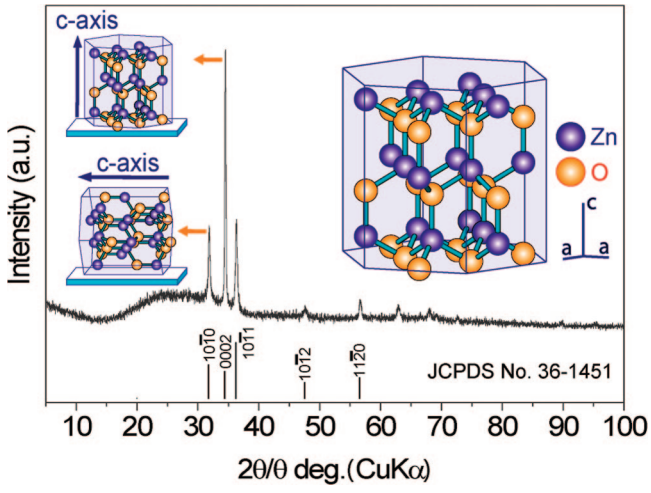

Figure 3. XRD diffraction pattern of multineedle ZnO particles having Ultrafine surface relief structure.

intensity from (0002) planes which are perpendicular to the *c*-axis would be caused from the crystalline ZnO particles which grew to elongate the *c*-axis. The particles have more stacks of (0002) crystal planes compared to that of (100) planes which are parallel to the *c*-axis or (101) planes and hence the intensity from (0002) planes was stronger than that from (100) or (101) planes.

ZnO grows to a hexagonal cylinder shape at low supersaturation degree because of its hexagonal crystal structure; however, ZnO grows to a multineedle shape at a high supersaturation degree which induces fast crystal growth. ZnO was thus grown to a multineedle shape in our solution in spite of its hexagonal crystal structure. The growth of ZnO was halted by a rapid decrease of supersaturation degree and removal of particles from the solution to obtain ZnO multineedle particles having an Ultrafine surface relief structure. The morphology of the ZnO particles was controlled by the fast crystal growth due to high supersaturation degree and by the suppression of crystal growth due to the rapid decrease of supersaturation degree and removal of particles from the solution.

Morphology Control of ZnO Particulate Films. ZnO particulate films showed a multineedle shape and were connected to each other by thin sheets (Figure 4a−c). The morphology of the particles was similar to that of the particles prepared by immersion for 80 min to have a high specific surface area. Thin sheets had a thickness of 10−50 nm and width of 1−10 μm and were connected closely to particles with no clearance. The particulate films had continuous open pores ranging from several nanometers to 10 μm in diameter. The particulate films showed X-ray diffraction patterns of ZnO crystal with no additional phase (Figure 5). Diffraction peaks were very sharp, showing high crystallinity of the particulate films. The high intensity of 0002 would be caused by elongation of multineedle particles in the *c*-axis direction which increases the stacks of (0002) crystal planes.

ZnO multineedle particles having an Ultrafine surface relief structure were prepared at 60 °C in the white solution during the initial 80 min (Figure 1e). The supersaturation degree was high at the initial stage of the reaction due to the high concentration of ions. ZnO particles were then precipitated, making the bottom of the solution white and the solution itself clear. Ions were consumed to form ZnO particles and thus the ion concentration of the solution decreased rapidly. Thin sheets were formed at 25 °C in the clear solution after the formation of multineedle particles (Figure 1f). Solution temperature and supersaturation degree would influence precipitates. Conse-

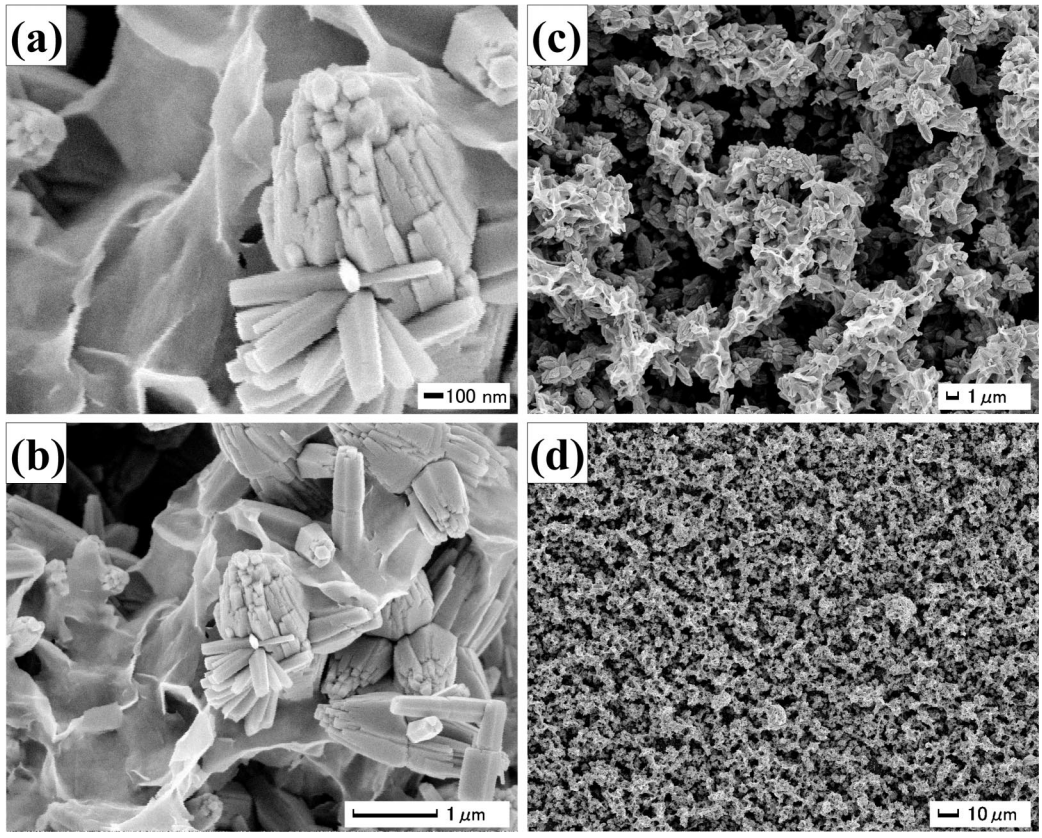

Figure 4. SEM micrograph (a−d) of ZnO particulate films constructed from ZnO multineedle particles and thin sheets.

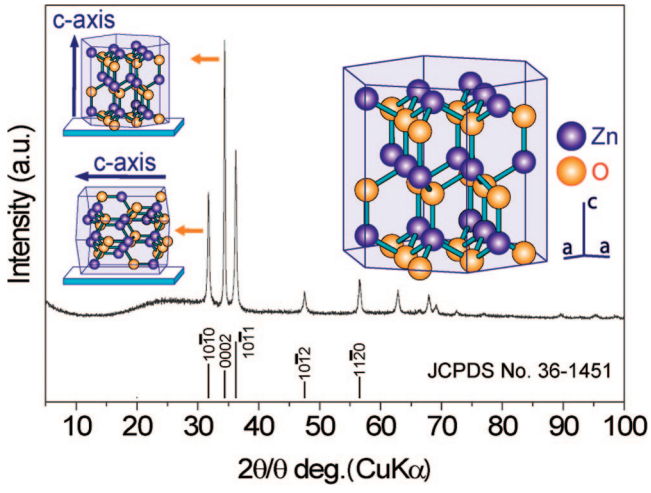

Figure 5. XRD diffraction pattern of ZnO particulate films constructed from ZnO multineedle particles and thin sheets.

quently, the particulate films constructed from multineedle particles and thin sheets were successfully fabricated by the two-step growth (Figure 1f).

For comparison, assemblies of thin sheets were prepared at air−liquid interfaces of the same solution we used in this study.[26] XRD patterns of the sheets were assigned to ZnO. The sheets had *c*-axis orientation parallel to the sheets, that is, in-plane *c*-axis orientation. TEM observations showed the sheets were dense polycrystals consisted of nanosized ZnO crystals. Electron diffraction pattern showed strong isotropic diffraction ring from (0002) planes. It suggested in-plane *c*-axis orientation of ZnO crystals which was consistent with XRD evaluations. Mechanical strength and electrical property would be affected by crystal orientation and microstructures. The sheets would have stronger mechanical strength compared to porous sheets because of their dense structure. They would have different electrical properties from randomly oriented sheets due to in-plane *c*-axis orientation, because ZnO has anisotropic electrical properties caused from anisotropic hexagonal crystal structure. The sheets prepared at air−liquid interfaces[26] would be similar to that prepared in the solutions (Figure 4) because both of them were prepared from the same solution and showed XRD patterns assigned to ZnO[26] (Figure 5). The sheets prepared in this study (Figures 4 and 5) would have similar mechanical and electrical properties to the sheets prepared at air−liquid interfaces.[26]

Thin sheets were transformed to particles and porous particulate films by annealing at 500 °C for 1 h in air. The sheets did not maintain their thin sheet shape due to high slimness and/or phase transformation. Thin sheets would be inorganic films containing Zn ions such as crystalline ZnO, amorphous ZnO, or zinc hydroxide and were transformed to porous ZnO particulate films by the annealing. Further investigation of the thin sheets would contribute to more precise morphology control of ZnO structure and further improvement of specific surface area. Additionally, precise evaluation of mechanical strength and electrical properties should be performed to clarify the potential of ZnO particulate films for sensors or solar cells and to produce guidelines for improving their properties.

Conclusions

We successfully fabricated multineedle ZnO particles having an Ultrafine surface relief structure by the precise control of crystal growth in an aqueous solution. The morphology of ZnO was further controlled for ZnO particu-

late films constructed from ZnO multineedle particles and thin sheets. The thin sheets connected particles to each other and with a substrate.

The morphology design and morphology control described here will facilitate the progress of crystal science for developing future advanced materials and devices.

References

(1) Gong, H.; Hu, J. Q.; Wang, J. H.; Ong, C. H.; Zhu, F. R. *Sens. Actuators B: Chem.* **2006**, *115*, 247–251.
(2) Moon, W. J.; Yu, J. H.; Choi, G. M. *Sens. Actuators B: Chem.* **2002**, *87*, 464–470.
(3) Chang, J. F.; Kuo, H. H.; Leu, I. C.; Hon, M. H. *Sens. Actuators B: Chem.* **2002**, *84*, 258–264.
(4) Tang, H. X.; Yan, M.; Zhang, H.; Li, S. H.; Ma, X. F.; Wang, M.; Yang, D. R. *Sens. Actuators B: Chem.* **2006**, *114*, 910–915.
(5) Shishiyanu, S. T.; Shishiyanu, T. S.; Lupan, O. I. *Sens. Actuators B: Chem.* **2005**, *107*, 379–386.
(6) Wagh, M. S.; Patil, L. A.; Seth, T.; Amalnerkar, D. P. *Mater. Chem. Phys.* **2004**, *84*, 228–233.
(7) Xu, J. Q.; Pan, Q. Y.; Shun, Y. A.; Tian, Z. Z. *Sens. Actuators B: Chem.* **2000**, *66*, 277–279.
(8) Paraguay, D. F.; Miki-Yoshida, M.; Morales, J.; Solis, J.; Estrada, L. W. *Thin Solid Films* **2000**, *373*, 137–140.
(9) Law, M.; Greene, L. E.; Johnson, J. C.; Saykally, R.; Yang, P. D. *Nat. Mater.* **2005**, *4*, 455–459.
(10) Baxter, J. B.; Aydil, E. S. *Appl. Phys. Lett.* **2005**, *86*, 53114.
(11) Katoh, R.; Furube, A.; Hara, K.; Murata, S.; Sugihara, H.; Arakawa, H.; Tachiya, M. *J. Phys. Chem. B* **2002**, *106*, 12957–12964.
(12) Karuppuchamy, S.; Nonomura, K.; Yoshida, T.; Sugiura, T.; Minoura, H. *Solid State Ionics* **2002**, *151*, 19–27.
(13) Keis, K.; Bauer, C.; Boschloo, G.; Hagfeldt, A.; Westermark, K.; Rensmo, H.; Siegbahn, H. *J. Photochem. Photobiol. A* **2002**, *148*, 57–64.
(14) Masuda, Y.; Kinoshita, N.; Sato, F.; Koumoto, K. *Cryst. Growth Des.* **2006**, *6*, 75–78.
(15) Kasuga, T.; Hiramatsu, M.; Hoson, A.; Sekino, T.; Niihara, K. *Adv. Mater.* **1999**, *11*, 1307-+
(16) Oaki, Y.; Imai, H. *J. Am. Chem. Soc.* **2004**, *126*, 9271–9275.
(17) Xia, Y. N.; Yang, P. D.; Sun, Y. G.; Wu, Y. Y.; Mayers, B.; Gates, B.; Yin, Y. D.; Kim, F.; Yan, Y. Q. *Adv. Mater.* **2003**, *15*, 353–389.
(18) Masuda, Y.; Saito, N.; Hoffmann, R.; De Guire, M. R.; Koumoto, K. *Sci. Tech. Adv. Mater.* **2003**, *4*, 461–467.
(19) Masuda, Y.; Ieda, S.; Koumoto, K. *Langmuir* **2003**, *19*, 4415–4419.
(20) Masuda, Y.; Jinbo, Y.; Yonezawa, T.; Koumoto, K. *Chem. Mater.* **2002**, *14*, 1236–1241.
(21) Nakanishi, T.; Masuda, Y.; Koumoto, K. *Chem. Mater.* **2004**, *16*, 3484–3488.
(22) Peng, W. Q.; Qu, S. C.; Cong, G. W.; Wang, Z. G. *Cryst. Growth Des.* **2006**, *6*, 1518–1522.
(23) Lin, Y. R.; Yang, S. S.; Tsai, S. Y.; Hsu, H. C.; Wu, S. T.; Chen, I. C. *Cryst. Growth Des.* **2006**, *6*, 1951–1955.
(24) Zhang, H.; Yang, D. R.; Li, D. S.; Ma, X. Y.; Li, S. Z.; Que, D. L. *Cryst. Growth Des.* **2005**, *5*, 547–550.
(25) Liu, K. H.; Lin, C. C.; Chen, S. Y. *Cryst. Growth Des.* **2005**, *5*, 483–487.
(26) Masuda, Y.; Kato, K. *Cryst. Growth Des.* **2008**, *8*, 275–279.

CG060607C